Original Article

Nuclear factor erythroid 2-related factor 2 alleviates lung endothelial cells injury by inhibition of ferroptosis

Xiaotong Yin, Chongbing Yan, Bowen Weng, Hao Luo, Cheng Cai

Department of Neonatology, Shanghai Children's Hospital, School of Medicine, Shanghai Jiao Tong University, Shanghai, China

Contributions: (I) Conception and design: C Cai, X Yin, C Yan; (II) Administrative support: C Cai; (III) Provision of study materials or patients: C Cai; (IV) Collection and assembly of data: X Yin, C Yan, B Weng; (V) Data analysis and interpretation: X Yin, B Weng, H Luo; (VI) Manuscript writing: All authors; (VII) Final approval of manuscript: All authors.

Correspondence to: Cheng Cai, MD, PhD. Department of Neonatology, Shanghai Children's Hospital, School of Medicine, Shanghai Jiao Tong University, 355 Luding Road, Shanghai 200062, China. Email: caic@shchildren.com.cn.

Background: In recent years, the survival rate of preterm infants has significantly improved due to the application of pulmonary surfactant (PS) and advancements in lung-protective mechanical ventilation strategies. However, this has been accompanied by an increased incidence of complications, particularly lung diseases triggered by elevated reactive oxygen species (ROS) induced by hyperoxia. The primary mechanism of hyperoxic lung injury (HLI) involves the excessive production of ROS within cells and the aggregation of inflammatory cells. Currently, no effective prevention or treatment methods are available. Ferroptosis, a newly identified form of cell death, is closely linked to ROS accumulation and is likely involved in HLI. Nuclear factor erythroid 2-related factor 2 (*Nrf2*) regulates both HLI and ferroptosis, and targeting *Nrf2* to inhibit ferroptosis may represent a key therapeutic approach for treating HLI. This study aimed to investigate the involvement of ferroptosis in HLI and to elucidate the regulatory role of *Nrf2*.

Methods: We employed the human pulmonary microvascular endothelial cell (HPMEC) model of hyperoxia exposure and corresponding intervention groups. Mitochondrial morphological alterations within HPMECs exposed to hyperoxia and various control groups were examined using transmission electron microscopy (TEM). Cell viability was assessed via the Cell Counting Kit-8 (CCK-8) assay, whereas intracellular ROS levels were quantified using the dichlorodihydrofluorescein diacetate (DCFH-DA) probe. Furthermore, the expression levels of *GPX4* and *Nrf2* were analyzed through quantitative polymerase chain reaction (qPCR) and western blot techniques.

Results: Relative to the control group, the HPMECs subjected to hyperoxic conditions exhibited diminished viability, heightened ROS levels, decreased *GPX4* expression, and increased *Nrf2* expression. These cells also demonstrated mitochondrial morphological alterations characteristic of ferroptosis, including reduced mitochondrial cristae and shrinkage. The application of a ferroptosis inhibitor mitigated cellular damage, lipid peroxidation, and the morphological manifestations of mitochondrial ferroptosis, whereas *Nrf2* inhibitor ML385 reversed this effect.

Conclusions: Ferroptosis appears to contribute to the pathogenesis of HLI, with *Nrf2* serving a protective function by mitigating ferroptosis.

Keywords: Ferroptosis; hyperoxic lung injury (HLI); glutathione peroxidase4; nuclear factor erythroid 2-related factor 2 (*Nrf2*)

Submitted Jul 26, 2024. Accepted for publication Nov 05, 2024. Published online Nov 26, 2024.
doi: 10.21037/tp-24-287
View this article at: https://dx.doi.org/10.21037/tp-24-287

Introduction

Oxygen therapy is a prevalent treatment modality for preterm infants, yet sustained exposure to elevated oxygen levels can inflict significant pulmonary damage, potentially culminating in fatality (1). With advancements in neonatal treatment and care enhancing the survivability of preterm infants, there has been a concomitant rise in the prevalence of hyperoxia-associated conditions such as bronchopulmonary dysplasia (BPD) and acute respiratory distress syndrome (ARDS). The vulnerability of preterm infants to oxidative injury is heightened due to their underdeveloped organ systems and diminished antioxidative defense mechanisms, underscoring the critical demand for therapeutic interventions targeting oxidative stress-induced disease.

Introduced by Dixon in 2012, ferroptosis denotes an iron-dependent form of cell death triggered by lipid peroxidation (2). Distinct from traditional cell death paradigms, ferroptosis exhibits unique morphological, biochemical, and genetic characteristics, the state of which is marked by an escalation in cellular lipid reactive oxygen species (ROS), oxidative by-products, and glutathione metabolism derivatives, such as malondialdehyde (MDA) and glutathione peroxidase (GPx) (3). Additionally, ferroptosis exhibits unique distinctive morphological changes such as cell membrane rupture, mitochondrial diminution, heightened membrane density, and the diminution or disappearance of mitochondrial cristae; these features can render it a potential biomarker for detection (4). *GPX4*, a pivotal antioxidative enzyme, preserving redox homeostasis by curbing lipid peroxidation and neutralizing phospholipid hydroperoxides, is also a key regulatory factor for ferroptosis (5). *Nrf2*, an antioxidative transcription factor, orchestrates the activation of an array of downstream antioxidative genes, including *GPX4*, concurrently diminishing intracellular ROS production and moderating iron assimilation, thereby significantly influencing ferroptosis regulation. Recent inquiries into ferroptosis have illuminated its contribution to the pathogenesis of diverse diseases, such as ischemia-reperfusion injury, cancer, cardiovascular, and respiratory ailments (4-6). The involvement of ferroptosis in hyperoxic lung injury (HLI) is progressively being disclosed, with empirical evidence indicating elevated ferroptosis markers in neonatal rat models of acute lung injury induced by hyperoxia, intimating its potential role in the pathophysiological trajectory of HLI (7). Notwithstanding, literature on the modulatory capacity of *Nrf2* over ferroptosis in ameliorating HLI remains scant. This investigation aimed to delineate the regulatory impact of *Nrf2* on ferroptosis in hyperoxia-induced lung injury using a human pulmonary microvascular endothelial cell (HPMEC) hyperoxia exposure model. We present this article in accordance with the MDAR reporting checklist (available at https://tp.amegroups.com/article/view/10.21037/tp-24-287/rc).

Highlight box

Key findings

- Ferroptosis appears to contribute to the pathogenesis of hyperoxic lung injury (HLI), with *Nrf2* playing a protective role by mitigating ferroptosis.

What is known and what is new?

- The confirmed forms of cell damage involved in HLI include autophagy, apoptosis, epithelial mesenchymal transition, and opening of intercellular connections.
- This investigation found that the regulatory impact of *Nrf2* on ferroptosis in HLI.

What is the implication, and what should change now?

- This study has discovered new forms of cell death in the process of HLI, providing insights for further understanding the underlying mechanisms of HLI and developing new treatment methods.

Methods

Reagents and materials

HPMECs were purchased from American Type Culture Collection (ATCC; Manassas, VA, USA) catalog number: CRL-3244. The chemical inhibitors Ferrostatin-1 (Fer-1) and ML385 were purchased from Shanghai Haoyuan Pharmaceutical Co. Ltd. (Shanghai, China). Antibodies against GPX4 (14432-1-AP), GADPH (60004-1-1), and Nrf2 (16396-1-AP) were obtained from Suzhou Meilun Biotechnology Co. Ltd. (Suzhou, China). Horseradish peroxidase (HRP)-conjugated goat anti-mouse IgG (H+L) (A0216) and goat anti-rabbit IgG (H+L) (A0208), along with the Cell Counting Kit-8 (CCK-8) assay kit, were supplied by Shanghai Biyun Tian Biotechnology Co. Ltd. (Shanghai, China). Transmission electron microscopy (TEM) analyses were performed using apparatus from Wuhan Sevier Biotechnology Co. Ltd. (Wuhan, China).

Development and grouping of the HPMECs hyperoxia model

Experimental setup logarithmically growing HPMEC cells

Table 1 Primer sequence for qPCR

Gene	Primer orientation	Primer sequence (5'-3')
Nrf2	Forward	TCCAGTCAGAAACCAGTGGAT
	Reverse	GAATGTCTGCGCCAAAAGCTG
GPX4	Forward	GAGGCAAGACCGAAGTAAACTAC
	Reverse	CCGAACTGGTTACACGGGAA
GAPDH	Forward	AGGTCGGTGTGAACGGATTTG
	Reverse	TGTAGACCATGTAGTTGAGGTCA

qPCR, quantitative polymerase chain reaction; *Nrf2*, nuclear factor erythroid 2-related factor 2; *GPX4*, glutathione peroxidase 4; *GAPDH*, glyceraldehyde-3-phosphate dehydrogenase.

were harvested and counted, then seeded uniformly in 96-well plates at a density of 5×10^4 cells per well, and cultured under standard conditions for 24 hours. The cultured cells were then randomly divided into four groups: control group, hyperoxia group, ferroptosis inhibitor group, and *Nrf2* inhibitor group. Control group cells were cultured under standard conditions; the hyperoxia model group was cultured in a hypoxic chamber continuously flushed with 95% oxygen for 5 minutes; the ferroptosis inhibitor group was cultured in a hypoxic chamber continuously flushed with 95% oxygen for 5 minutes and 10 μM of Fer-1 was added to the culture medium; the Nrf2 inhibitor group received 10 μM of ML385 under the same conditions. All groups were incubated at 37 ℃. Cells were collected from each group at 24 and 48 hours for subsequent experiments. The experiment was repeated independently three times.

Assessment of cell viability via CCK-8 assay

CCK-8 was employed to evaluate cell viability. Cell suspensions were allocated into a 96-well plate at 24 and 48 hours post-treatment. Subsequent to the experimental treatment, the culture medium was removed, and 100 μL of CCK-8 solution was introduced into each well. The absorbance at 450 nm was measured with a microplate reader following a 2-hour incubation in a darkened cell culture incubator. The optical density (OD) readings obtained from the microplate reader were utilized to compute the survival rates of the cells.

Quantification of intracellular ROS via flow cytometry

Intracellular ROS concentrations in HPMECs for all experimental groups were quantified employing a fluorescent ROS detection kit. Cells were enzymatically dissociated using trypsin, followed by phosphate-buffered saline (PBS) washes. The fluorescent probe dichlorodihydrofluorescein diacetate (DCFH-DA) was prepared at a concentration of 10 μM in serum-free medium, diluted at a 1:1,000 ratio. The cells were incubated in darkness at 37 ℃ for 30 minutes, intermittently agitating the mixture every 3–5 minutes to ensure uniform probe-cell interaction. Subsequent to incubation, cells underwent triple PBS washes in preparation for flow cytometric analysis.

Real-time fluorescent quantitative polymerase chain reaction (qPCR) for the analysis of GPX4 and Nrf2 messenger RNA expression in HPMECs

(I) RNA isolation: HPMECs were harvested from each experimental group, with total RNA extracted utilizing the TRIzol protocol, subsequent to treatments reflective of diverse experimental conditions.

(II) Synthesis of complementary DNA: the reaction mixture was prepared in 0.2 mL PCR tubes. Tubes were initially held at 25 ℃ for 5 minutes, incubated at 42 ℃ for 30 minutes, denatured at 85 ℃ for 5 minutes, then conserved at 4 ℃.

(III) Real-time qPCR (RT-qPCR): initial denaturation at 95 ℃ for 30 seconds, followed by 40–45 cycles of 95 ℃ for 5 seconds and 60 ℃ for 34 seconds, and then melting curve analysis at 95 ℃ for 15 seconds, 60 ℃ for 60 seconds, and 95 ℃ for 15 seconds. Amplification was monitored on the system.

(IV) Data interpretation: relative gene expression was quantified employing the $2^{-\Delta\Delta CT}$ method. Primers specifically designed for this analysis were synthesized by Shanghai Ji Ke Biochemical Co., Ltd. (Shanghai, China). Details regarding the primer sequences utilized for qPCR are documented in *Table 1*.

Western blot analysis for GPX4 and Nrf2 protein levels in HPMECs

Sodium dodecyl sulfacte polyacrylamide gel electrophoresis (SDS-PAGE) gels were prepared and the electrophoresis tank was filled with buffer. Electrophoresis commenced at 80 V for 15 minutes, followed by 120 V for 55–80 minutes, before proteins were semi-transferred to a polyvinylidene difluoride (PVDF) membrane. The membrane was blocked

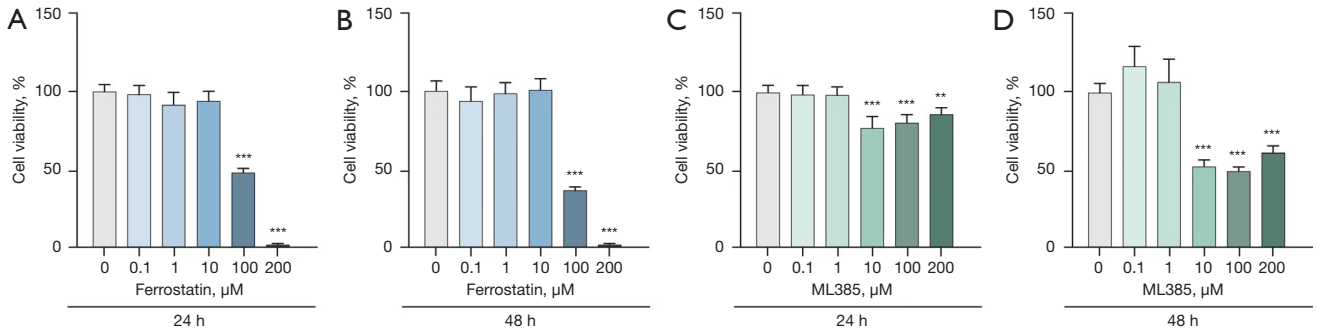

Figure 1 CCK-8 experiment explores the appropriate dosage of Ferrostatin and ML385 (24 and 48 h). **, P<0.01 *vs.* 0 μM; ***, P<0.001 *vs.* 0 μM. CCK-8, Cell Counting Kit-8.

with 5% skim milk in tris-buffered saline (TBS) solution for one hour. The membrane was then incubated overnight at 4 ℃ with the primary antibody (HRP-conjugated goat anti-mouse antibody). Following several washes with phosphate-buffered saline with Tween 20 (PBST) buffer, the secondary antibody (HRP-conjugated goat anti-rabbit antibody) was applied and incubated at room temperature for 2 hours. The membrane was washed with PBS buffer, treated with electrochemiluminescence (ECL) liquid for 2 minutes, and developed using imaging equipment. Band grayscale values were assessed using Image J software (National Institutes of Health, Bethesda, MD, USA).

Evaluation of mitochondrial morphology via TEM

HPMECs were exposed to Fer-1 and ML385 at a 10 μM concentration for durations of 24 and 48 hours, in addition to undergoing hyperoxia treatment for 24 and 48 hours. Cells from each treatment group were subsequently gathered for ultrastructural examination under TEM to assess mitochondrial morphology.

Statistical methodology

The software package SPSS 23.0 (IBM Corp., Armonk, NY, USA) was employed for data analysis. Normally distributed quantitative data were presented as the mean ± standard deviation ($\bar{x}\pm s$). The two-sample *t*-test was used for comparison between two distinct groups, whereas analysis of variance (ANOVA) was applied for comparisons across multiple groups. A P value of less than 0.05 was interpreted as indicative of statistical significance.

Results

Determination of optimal drug concentrations using CCK-8

The optimal drug concentrations for the iron death inhibitor (Fer-1) and the *Nrf2* inhibitor (ML385) were evaluated by their effects on HPMEC.

Cells were treated with 0, 0.1, 1, 100, and 200 μM of Fer-1 and ML385 for 24 and 48 hours, and cell viability was assessed by measuring the OD. It was found that 10 μM Fer-1 did not reduce cell viability at 24 and 48 hours (*Figure 1A*,*1B*); however, 10 μM ML385 significantly decreased cell survival compared to control (*Figure 1C*,*1D*), with statistically significant differences. Future experiments will use a concentration of 10 μM for both Fer-1 and ML385 (*Figure 1*).

Hyperoxia exposure induces ferroptosis in HPMECs, Fer-1 suppresses ferroptosis, and mitigates hyperoxia-induced cellular damage

To investigate the impact of hyperoxia exposure on cells, all groups except the control were cultured under conditions with an oxygen volume fraction of 95% oxygen, with different intervention reagents added. The results were observed at 24 and 48 hours, respectively. The findings revealed a time-dependent decrease in cell viability following hyperoxia exposure (*Figure 2*), indicating that such exposure leads to cellular damage and death. To assess whether ferroptosis contributes to the cell damage induced by hyperoxia exposure, cells were treated with 10 μM of the ferroptosis inhibitor, Fer-1, alongside hyperoxia. Compared to the hyperoxia group, cells treated with Fer-1 exhibited

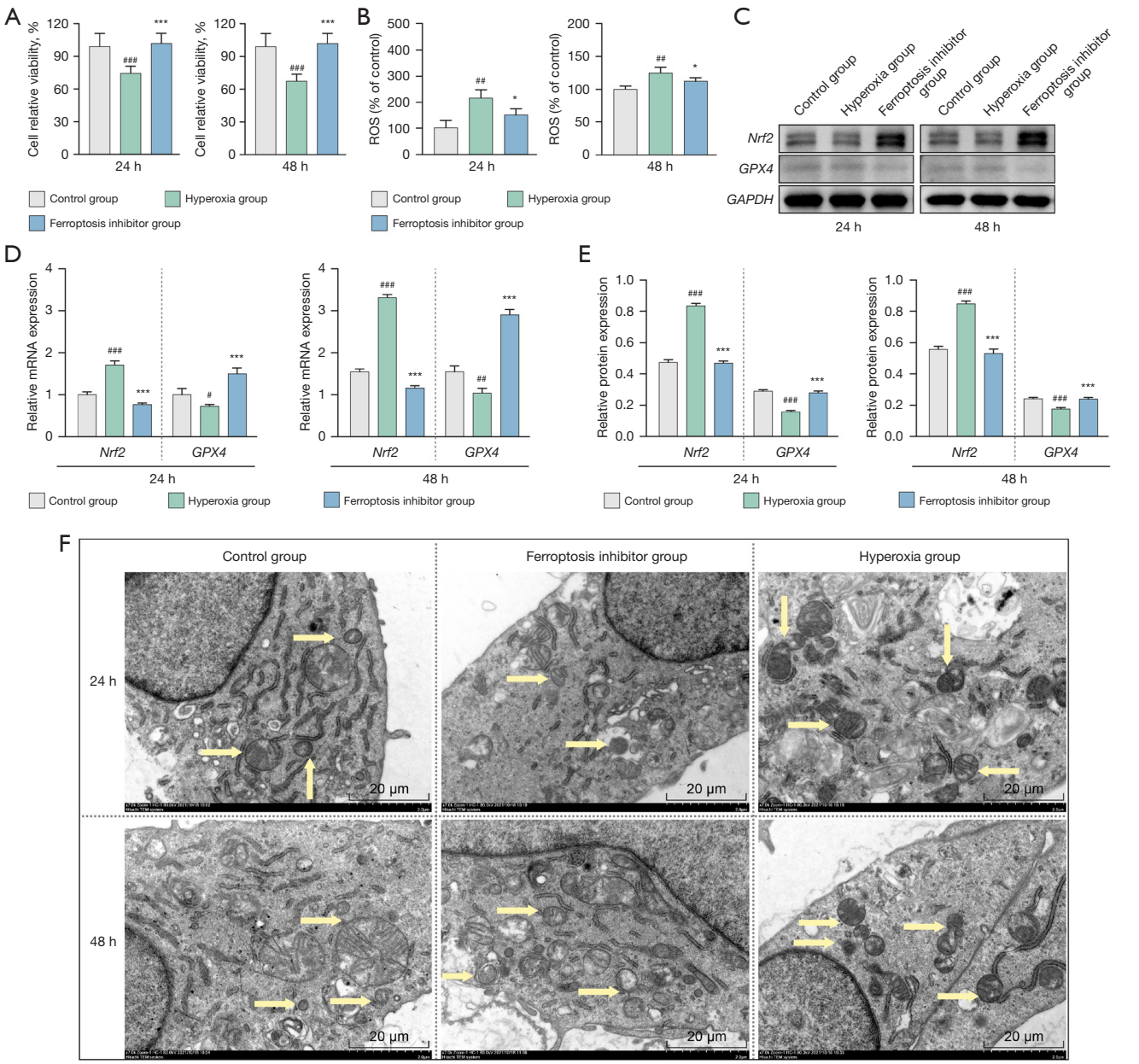

Figure 2 Comparing the effects of hyperoxia and ferroptosis inhibitor on HPMECs. CCK-8 was employed to evaluate cell viability. The cell viability was significantly lower in the hyperoxia group than in the control group, and it was higher in the ferroptosis inhibitor group than in the hyperoxia group (A). Flow cytometry assessment of cellular ROS levels in each group. ROS content within HPMECs following hyperoxia exposure is increased, and it was increased after Fer-1 treatment (B). Images of protein expression levels of two groups were analyzed by western blot (C). RT-PCR and Western blot analysis of *Nrf2* and *GPX4* mRNA and protein expression levels in each group. *Nrf2* expression levels were significantly higher in the hyperoxia group than in the control group, but significantly lower in the ferroptosis inhibitor group than in the hyperoxia group. The changes in *GPX4* expression levels are the opposite (D,E). Observation of mitochondrial morphology changes in HPMECs of each group using transmission electron microscopy (F). Compared to the control group, $^{###}$, P<0.001; $^{##}$, P<0.01; $^{#}$, P<0.05. Compared to the hyperoxia group, ***, P<0.001; *, P<0.05. The yellow arrows point to the mitochondria. ROS, reactive oxygen species; Nrf2, nuclear factor-erythroid 2-related factor 2; GPX4, glutathione peroxidase 4; GAPDH, glyceraldehyde-3-phosphate dehydrogenase; mRNA, messenger RNA; HPMECs, human pulmonary microvascular endothelial cells; CCK-8, Cell Counting Kit-8; Fer-1, Ferrostatin-1; RT-PCR, reverse transcription polymerase chain reaction.

significantly increased viability (*Figure 2A*). Elevated ROS levels are indicative of cellular ferroptosis. DCFH-DA fluorescent probe analysis revealed an increase in ROS content within HPMECs following hyperoxia exposure, with a notable reduction in ROS content observed after Fer-1 treatment (*Figure 2B*). *GPX4* is a crucial intracellular antioxidant enzyme and a key inhibitor of ferroptosis. Post hyperoxia exposure, cellular *GPX4* messenger RNA (mRNA; 24 h: 0.750±0.010 *vs.* 1.010±0.160, 48 h: 0.690±0.050 *vs.* 1.000±0.070) and protein (24 h: 0.160±0.010 *vs.* 0.290±0.010, 48 h: 0.190±0.010 *vs.* 0.250±0.010) expression decreased, whereas it significantly increased upon Fer-1 addition (mRNA 24 h: 1.520±0.110 *vs.* 0.750±0.010, 48 h: 1.880±0.050 vs.0.690±0.050, protein 24 h: 0.290±0.010 *vs.* 0.160±0.010, 48 h: 0.250±0.004 *vs.* 0.190±0.010) (*Figure 2C-2E*). Furthermore, TEM revealed characteristic alterations associated with ferroptosis in HPMECs after hyperoxia exposure, including reduced mitochondrial cristae and shrinkage; the electron density of mitochondria also decreased (*Figure 2F*). Notably, adding Fer-1 resulted in more intact mitochondria within HPMECs (*Figure 2F*). In summary, Fer-1 effectively attenuates HPMEC cell damage under hyperoxia exposure, mitigates ROS generation, and enhances *GPX4* expression, underscoring the involvement of ferroptosis in HLI.

Nrf2 suppression aggravates hyperoxia-induced damage and intracellular ferroptosis in HPMECs

To investigate the influence of *Nrf2* on hyperoxia-induced damage in HPMECs, cells were treated with 10 μM ML385 in addition to hyperoxia exposure. As illustrated in *Figure 3*, the results from the fluorescent probe DCFH-DA demonstrated a significant decrease in cell viability post-ML385 treatment (*Figure 3A*). Flow cytometry revealed elevated intracellular ROS levels (*Figure 3B*), whereas *GPX4* mRNA (24 h: 0.600±0.030 *vs.* 0.750±0.010, 48 h: 0.590±0.003 *vs.* 0.690±0.050) and protein (24 h: 0.150±0.001 *vs.* 0.160±0.010, 48 h: 0.180±0.001 *vs.* 0.190±0.010) expression within cells decreased following ML385 treatment (*Figure 3C-3E*). Moreover, observation under TEM revealed more pronounced reductions in mitochondrial cristae and shrinkage in HPMECs treated with the *Nrf2* inhibitor compared to the hyperoxia group (*Figure 3F*). These results indicate that ML385 inhibits intracellular *Nrf2* expression, exacerbating hyperoxia-induced cellular damage and the occurrence of intracellular ferroptosis.

Discussion

Administering high concentrations of oxygen is a prevalent method for treating certain respiratory conditions. Nonetheless, surpassing the adaptive capacity of the human body may precipitate lung injury, a phenomenon corroborated by numerous animal studies. Long term exposure to high oxygen can precipitate immune dysfunction, metabolic disturbances, and compromise the integrity of the alveolar barrier, these pathophysiological changes are evident histologically as alveolar hemorrhage, vascular leakage, inflammatory cell infiltration, and pulmonary fibrosis (8). Although the precise molecular underpinnings of HLI remain to be fully delineated, signaling pathways and activation of pro-inflammatory cytokines have emerged as pivotal contributory factors during high oxygen exposure. Our investigation further substantiates that heightened oxygen exposure leads to an escalation in ROS levels and a reduction in GPX4 content within HPMEC, culminating in cellular structural disruption and elevated mortality rates. These results indicate that redox imbalance is a key factor in HLI.

Our research indicates that high oxygen exposure reduces cell viability and elevates mortality in HPMEC cells, whereas introducing the ferroptosis inhibitor Fer-1 markedly improves cell viability and lowers mortality rates.

Moreover, Fer-1 treatment diminishes ROS levels and augments *GPX4* expression, thereby curtailing he buildup of intracellular peroxides. Observations through TEM disclosed that Fer-1 could reverse the mitochondrial alterations in HPMEC cells post high oxygen exposure, indicative of ferroptosis. These findings underscore the role of ferroptosis in lung injuries attributed to high oxygen levels and posit that mitigating ferroptosis can ameliorate HLI. Ferroptosis is an iron-dependent, regulated cell death mechanism characterized by several hallmark features, including disruptions in iron homeostasis, compromised oxidative stress defenses, and anomalous lipid peroxidation. After high oxygen exposure, cells generate a significant amount of oxygen-based radicals. Accumulation of membrane lipid peroxides to toxic levels activates the ferroptosis pathway, compromising the integrity of the plasma membrane, leading to cell fragmentation and the leakage of intracellular components, resulting in lung injury (9). The process can be pharmacologically inhibited by the ferroptosis inhibitor (Fer-1). Similarly, studies indicate that seawater drowning can cause severe oxidative stress, leading to ferroptosis, which results in acute lung

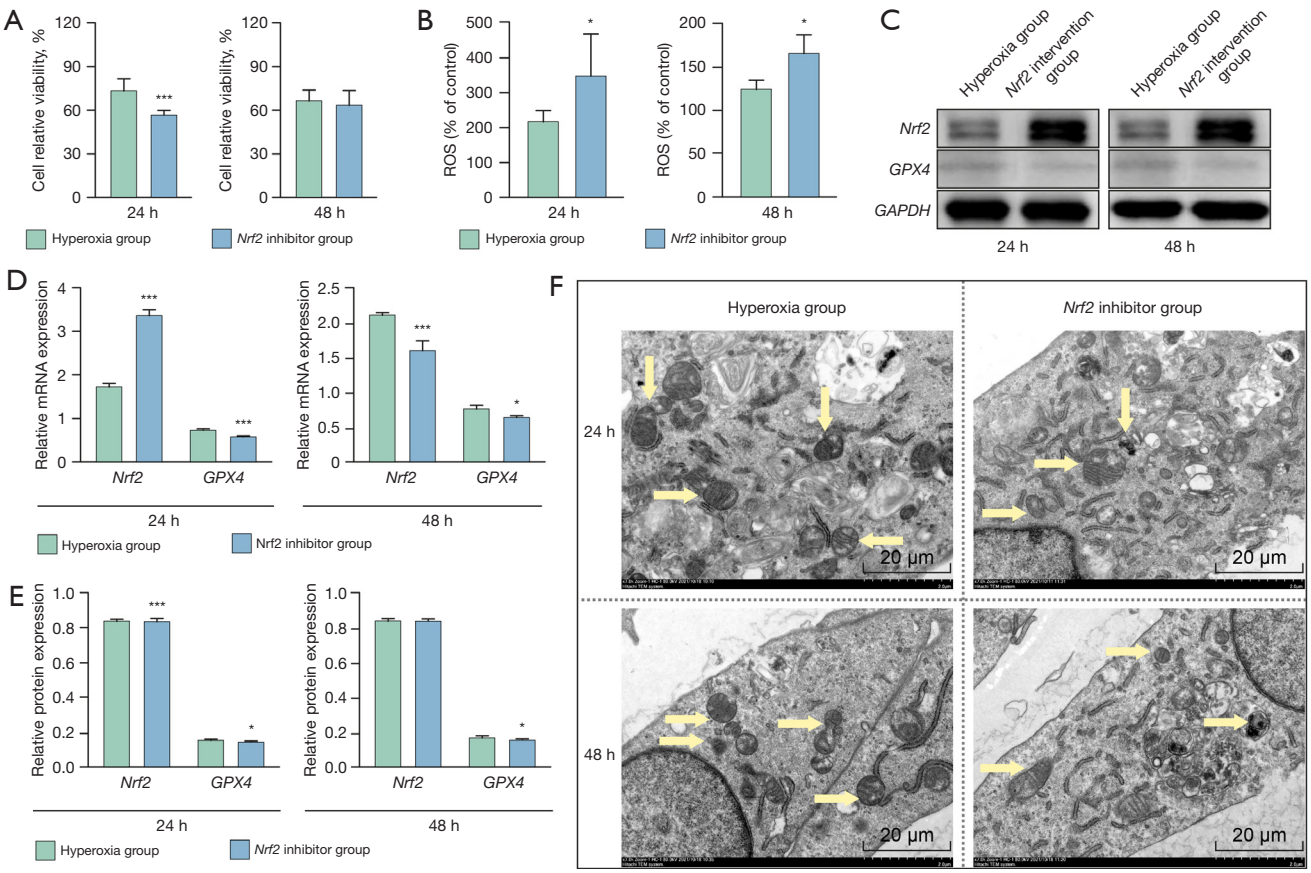

Figure 3 Comparing the effects of hyperoxia and Nrf2 inhibitor on HPMECs. CCK-8 was employed to evaluate cell viability. The cell viability was lower in the *Nrf2* inhibitor group than in the hyperoxia group (A). Flow cytometry assessment of cellular ROS levels in each group. ROS content within HPMECs was increased after *Nrf2* inhibitor treatment (B). Images of protein expression levels of two groups were analyzed by western blot (C). RT-PCR and western blot analysis of *Nrf2* and *GPX4* mRNA and protein expression levels in two groups. Compared to the hyperoxia group, the level of *Nrf2* mRNA was significantly increased at 24 h and decreased at 48 h, but the protein expressions of *Nrf2* between two groups were similar. Compared to the hyperoxia group, the mRNA and protein expressions of *GPX4* at 24 h and 48 h in the *Nrf2* inhibitor group were all decreased (D,E). Observation of mitochondrial morphology changes in HPMECs of each group using transmission electron microscopy (F). Compared to the hyperoxia group, ***, P<0.001; *, P<0.05. The yellow arrows point to the mitochondria. ROS, reactive oxygen species; *Nrf2*, nuclear factor-erythroid 2-related factor 2; GPX4, glutathione peroxidase 4; GAPDH, glyceraldehyde-3-phosphate dehydrogenase; HPMECs, human pulmonary microvascular endothelial cells; CCK-8, Cell Counting Kit-8; RT-PCR, reverse transcription polymerase chain reaction.

injury. Inhibiting ferroptosis can mitigate the lung injury induced by seawater drowning (10). In an acute lung injury model due to intestinal ischemia reperfusion, increased peroxides was shown to trigger ferroptosis, and inhibiting ferroptosis served a protective function (11).

This study demonstrates that high oxygen exposure prompts an upsurge in *Nrf2* expression in HPMEC cells, which, upon administration of ML385, declines within 48 hours, paralleled by an increase in intracellular ROS and a decrease in *GPX4* expression, aggravating the cellular damage induced by high oxygen levels. The introduction of ML385 accentuated mitochondrial changes akin to ferroptosis, such as diminished mitochondrial cristae and contraction, more so than in the high oxygen-exposed group alone. These observations suggest that *Nrf2* serves as a deterrent to ferroptosis, thereby mitigating lung damage incurred from high oxygen exposure. The p62-Keap1-NRF2 axis is instrumental

in modulating oxidative stress. Prior studies have shown that this pathway upregulates genes involved in iron and ROS metabolism such as oxidoreductases, heme oxygenase-1, and ferritin-related enzymes, which serve as negative regulators of ferroptosis (12). Therefore, upregulating the expression of *Nrf2* can inhibit ferroptosis and have a protective effect on the body. For instance, salidroside's activation of the Nrf2/GPX4 axis inhibits neuronal ferroptosis, mitigating cognitive deficits associated with Alzheimer's disease (13). Similarly, quercetin ameliorates diabetic nephropathy by deactivating ferroptosis through the Nrf2/HO-1 signaling pathway (14).

Conclusions

This investigation corroborates that *Nrf2* can counteract ferroptosis, thereby alleviating HLI, and enriches our comprehension of the underlying mechanisms of HLI and its therapeutic outlook. Nevertheless, additional research is imperative to delineate the precise regulatory mechanisms by which *Nrf2* influences ferroptosis and HLI.

Acknowledgments

The authors would like to thank the Cell Laboratory Centre, Shanghai Jike Medical Information Technology Company for assistance with the experiments.

Funding: This study was supported by grants from 2023 "Science and Technology Rejuvenating Mongolia" Shanghai Jiaotong University Action Plan special project (No. 2023XYJG0001-01-09); and 2023 Hospital-level Clinical Research Training Program of Shanghai Children's Hospital (No. 2023YLY02).

Footnote

Reporting Checklist: The authors have completed the MDAR reporting checklist. Available at https://tp.amegroups.com/article/view/10.21037/tp-24-287/rc

Data Sharing Statement: Available at https://tp.amegroups.com/article/view/10.21037/tp-24-287/dss

Peer Review File: Available at https://tp.amegroups.com/article/view/10.21037/tp-24-287/prf

Conflicts of Interest: All authors have completed the ICMJE uniform disclosure form (available at https://tp.amegroups.com/article/view/10.21037/tp-24-287/coif). The authors have no conflicts of interest to declare.

Ethical Statement: The authors are accountable for all aspects of the work in ensuring that questions related to the accuracy or integrity of any part of the work are appropriately investigated and resolved.

References

1. Kallet RH, Matthay MA. Hyperoxic acute lung injury. Respir Care 2013;58:123-41.
2. Dixon SJ, Lemberg KM, Lamprecht MR, et al. Ferroptosis: an iron-dependent form of nonapoptotic cell death. Cell 2012;149:1060-72.
3. Chen GH, Song CC, Pantopoulos K, et al. Mitochondrial oxidative stress mediated Fe-induced ferroptosis via the NRF2-ARE pathway. Free Radic Biol Med 2022;180:95-107.
4. Zhang Y, Xin L, Xiang M, et al. The molecular mechanisms of ferroptosis and its role in cardiovascular disease. Biomed Pharmacother 2022;145:112423.
5. Li D, Wang Y, Dong C, et al. CST1 inhibits ferroptosis and promotes gastric cancer metastasis by regulating GPX4 protein stability via OTUB1. Oncogene 2023;42:83-98.
6. Lee H, Zandkarimi F, Zhang Y, et al. Energy-stress-mediated AMPK activation inhibits ferroptosis. Nat Cell Biol 2020;22:225-34.
7. Jia D, Zheng J, Zhou Y, et al. Ferroptosis is Involved in Hyperoxic Lung Injury in Neonatal Rats. J Inflamm Res 2021;14:5393-401.
8. Aggarwal NR, D'Alessio FR, Tsushima K, et al. Moderate oxygen augments lipopolysaccharide-induced lung injury in mice. Am J Physiol Lung Cell Mol Physiol 2010;298:L371-81.
9. Dixon SJ, Pratt DA. Ferroptosis: A flexible constellation of related biochemical mechanisms. Mol Cell 2023;83:1030-42.

10. Qiu YB, Wan BB, Liu G, et al. Nrf2 protects against seawater drowning-induced acute lung injury via inhibiting ferroptosis. Respir Res 2020;21:232.
11. Dong H, Qiang Z, Chai D, et al. Nrf2 inhibits ferroptosis and protects against acute lung injury due to intestinal ischemia reperfusion via regulating SLC7A11 and HO-1. Aging (Albany NY) 2020;12:12943-59. Erratum in: Aging (Albany NY) 2023;15:10811-2.
12. Sun X, Ou Z, Chen R, et al. Activation of the p62-Keap1-NRF2 pathway protects against ferroptosis in hepatocellular carcinoma cells. Hepatology 2016;63:173-84.
13. Yang S, Wang L, Zeng Y, et al. Salidroside alleviates cognitive impairment by inhibiting ferroptosis via activation of the Nrf2/GPX4 axis in SAMP8 mice. Phytomedicine 2023;114:154762.
14. Feng Q, Yang Y, Qiao Y, et al. Quercetin Ameliorates Diabetic Kidney Injury by Inhibiting Ferroptosis via Activating Nrf2/HO-1 Signaling Pathway. Am J Chin Med 2023;51:997-1018.

(English Language Editor: J. Jones)

Cite this article as: Yin X, Yan C, Weng B, Luo H, Cai C. Nuclear factor erythroid 2-related factor 2 alleviates lung endothelial cells injury by inhibition of ferroptosis. Transl Pediatr 2024;13(11):1985-1993. doi: 10.21037/tp-24-287